Degree Course Life Technologies

Option Analytical Chemistry

Diploma 2008

Cindy Meyrat

Profiling of anionic metabolites using CE-qTOF-MS with bare fused silica capillaries

Professor   Dr. B. Markus LANGE

Expert   Dr. Urban FREY

Sion, March 2009

Profil de métabolites anioniques par CE-qTOF-MS au moyen de capillaires en silice vierge

Profiling of anionic metabolites using CE-qTOF-MS with bare fused silica capillaries

Objectif

L'approche *metabolomics* est devenue une stratégie importante afin de progresser dans la compréhension des divers aspects du métabolisme. Toutefois, la connaissance globale de l'ensemble des métabolites cellulaires représente un redoutable défi de part l'immense éventail de structures et de propriétés chimiques que possèdent ces composés. Le couplage de l'électrophorèse capillaire à la spectrométrie de masse est considéré comme étant une technique prometteuse pour le profil de métabolites polaires et ioniques ; composés qui jouent un rôle important dans de nombreux processus métaboliques.

De part le fait que le couplage de l'EC et du MS supprime la présence d'une vial de sortie, contrairement à l'EC classique, la séparation des métabolites anioniques se révèle ambitieuse. En effet, le EOF agit dans le sens opposé à celui de la mobilité electrophorétique des anions. L'emploi de capillaires dont les parois sont chargées positivement a été suggéré, mais cette approche souffre du coût très élevé des capillaires ainsi que de la courte durée d'utilisation de ceux-ci.

Résultats

Le travail présenté ici propose l'approche d'un profil métabolique par électrophorèse capillaire couplé à la spectrométrie de masse afin d'analyser des métabolites anioniques tels que acides organiques, sucres phosphates et dérivés de coenzyme A. Ceci en employant un capillaire en silice vierge, très bon marché et en profitant du EOF en direction de la cathode.

Ce travail est le premier à présenter la séparation de sept dérivés de coenzyme A par EC-MS.

Mots-clés

Profil de métabolites anioniques, électrophorèse capillaire-spectrométrie de masse, CE-QTOF, capillaire en silice vierge, acides organiques, sucres phosphates, dérivés de coenzyme A.

Objective

Metabolomics approaches have become an important strategy to gain insight into various aspects of metabolism. However, the comprehensive coverage of all cellular metabolites presents formidable challenges because of the immense range of structures and chemical properties. Capillary electrophoresis coupled to mass spectrometry is considered a promising technique for the profiling of polar and ionic metabolites, which play important roles in numerous metabolic processes.

Because the coupling of CE and MS eliminates the outlet vial, contrary to regular CE, the separation of anionic metabolites is challenging. The EOF acts in the opposite direction compared to the electrophoretic mobility of anions. The use of capillaries with positively charged surfaces has been suggested, but this approach suffers from high capillary prices and short capillary lifetimes.

Results

The present work introduces a metabolic profiling approach using capillary electrophoresis coupled to mass spectrometry to analyze anionic metabolites such as organic acids, sugar phosphates and coenzyme A derivatives, using an inexpensive bare fused silica capillary, by taking advantage of the EOF velocity towards the cathode.

This paper is the first to report the separation of seven coenzyme A derivatives by CE-MS.

Keywords

Anionic metabolites profiling, capillary electrophoresis-mass spectrometry, CE-QTOF, bare fused silica capillary, organic acids, sugar phosphates, coenzyme A derivatives.

Table of contents :

1 Introduction

1.1 Objectives

- Operate a brand new capillary electrophoresis-mass spectrometer (CE-qTOF)

- Develop a novel CE-MS method for the separation of anionic metabolites with relevance to central carbon metabolism

1.2 Metabolome analysis

Recent advances in genetic mapping and nucleotide sequencing have provided with the DNA blueprints of entire genomes. The challenge now is to unravel the function of the genes within these genomes. Metabolomics aims at generating a snapshot of all metabolites present in a sample and is considered key for understanding the correlation between genes and the phenotype of an organism. It is important to note that metabolites represent the highest hierarchy level in a biochemical system (closer to a phenotype than genes and enzymes). [1][2]

Metabolomics generally utilizes non-target approaches to cover large numbers of metabolites. Several approaches have employed analytical methods such as gas chromatography-mass spectrometry (GC-MS), high-performance liquid chromatography-mass spectrometry (HPLC-MS), and nuclear magnetic resonance (NMR). However, because of the wide range of metabolite properties, no single technique encompasses the entire metabolome. [3]

GC-MS confers very high performance but is limited to volatile metabolites and those that can be derivatized to yield volatiles. Moreover, methods may require complicated and time-consuming chemical derivatization. [4]
Reversed phase liquid chromatography is amenable to more types of compounds but is not viable for highly polar metabolites [5]. Ion-exchange chromatography coupled to MS is difficult as well, because of the high level of non–volatile salts in the mobile phase [4] preventing the ionization process. Excess salt can also interfere with the performance of the mass spectrometer by overloading the system with charged salt ions.
NMR is an attractive method for high throughput fingerprinting but it suffers of poor sensitivity and metabolome coverage [5].

Capillary electrophoresis (CE) is considered as a promising technique for the analysis of highly polar metabolites. Indeed, CE has several advantages: high resolution power, compounds can be analyzed without derivatization and a small sample quantity is sufficient for analysis. [3][6][7]

The recent direct coupling of capillary electrophoresis to electrospray ionization mass spectrometry (CE/ESI-MS), enabled by adapting the interface to the low flow of the CE by introducing a sheath flow, has emerged as a powerful analytical tool for the analysis of charged species analyses. CE confers efficient resolution and MS provides high selectivity and sensitivity [2][3][4][5][6].

1.3   Biochemical relevance of anionic metabolites

The key pathways for cellular energy production, such as the Citric acid cycle and Calvin cycle involve numerous anionic metabolites. Anionic metabolites also exist in many other pathways.

The citric acid cycle (catabolic pathway), Figure 1, completes the breakdown of glucose in the stages of cellular respiration by oxidizing the derivate of pyruvate to carbon dioxide. This step in the cellular energy production takes place within the mitochondrial matrix of eukaryotic cells and in the cytosol of prokaryotes. The cycle has eight steps with a different intermediate organic acid for each step of the reaction. [8]
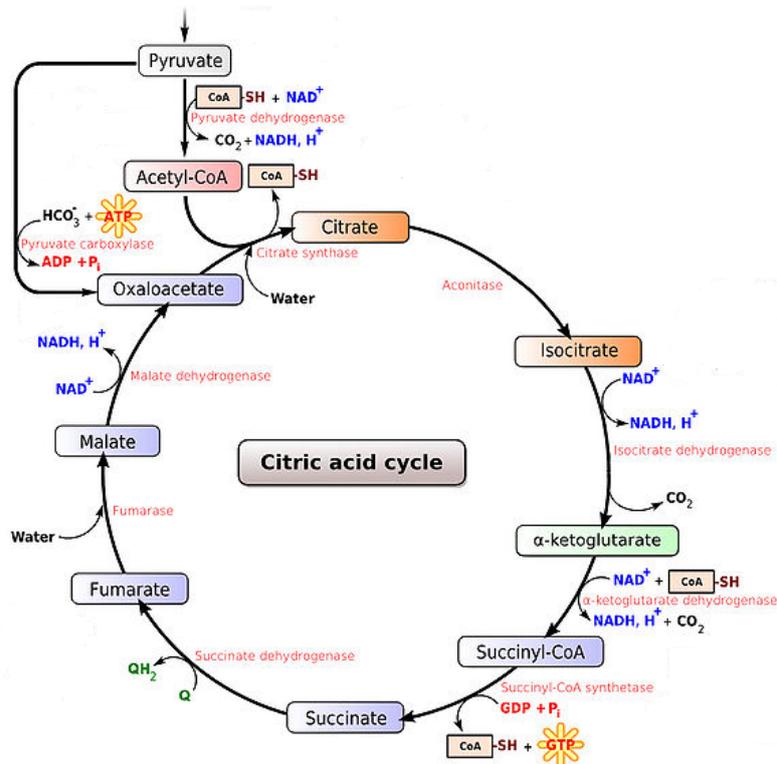
[http://en.wikipedia.org/wiki/Citric_acid_cycle]

Figure 1 : Citric acid cycle featuring different organic acids.

Acronyms: NADH, Nicotinamide adenine dinucleotide; GTP, Guanosine triphosphate; Q, coenzyme Q; ATP, adenosine triphosphate.

The Calvin cycle (anabolic pathway), Figure 2, builds carbohydrates from CO_2 and consumes energy. This cycle takes place in the stroma of chloroplasts in photosynthetic organisms and involves a sugar phosphates and related anionic metabolites. [8]

Coenzyme A (CoA) is a central metabolite in many metabolic processes and in the biosynthesis of some carbohydrates and lipids, as illustrated in Figure 3. This crossroad compound of cellular metabolism facilitates more than 100 chemical reactions [9]. CoA initiates the Citric acid cycle, which produces more than 90% of the energy in cellular processes [9] and is also involved in the metabolism of amino acids and isoprenoids.
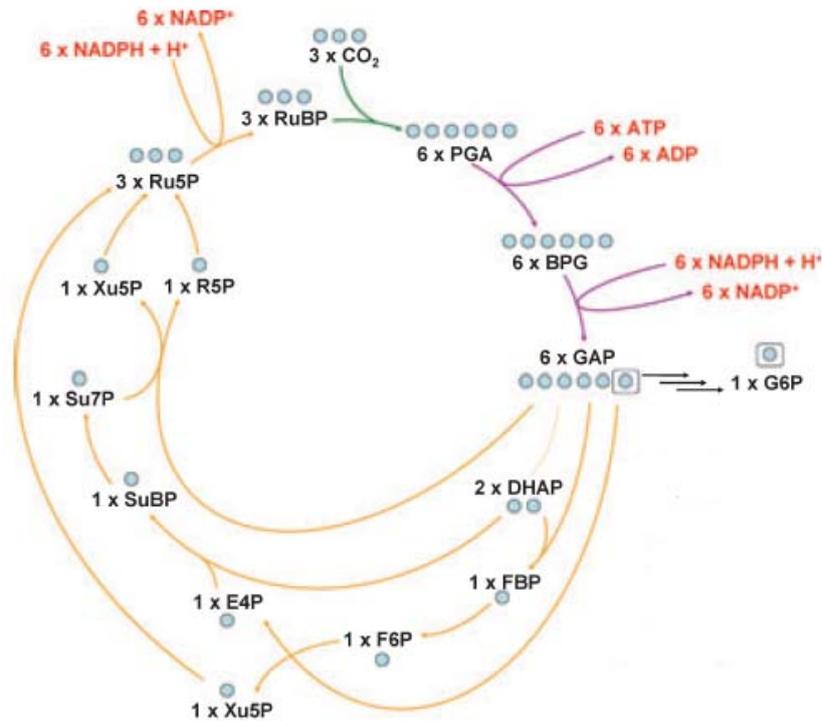
Figure 2 : Sugar phosphates of the Calvin Cycle, modified from [10].

Acronyms: BPG, 1,3-bisphosphoglycerate; DHAP, dihydroxyacetone phosphate; E4P, erythrose-4-phosphate; F6P, fructose-6-phosphate; GAP, glyceraldehyde-3-phosphate; G6P, glucose-6-phosphate; PGA, phosphoglycerate; R5P, ribose-5-phosphate; RuBP, ribulose-1,5-bisphosphate; SuBP, sedoheptulose-1,7-bisphosphate; Su7P, sedoheptulose-7-phosphate; Xu5P, xylulose-5-phosphate; NADH, Nicotinamide adenine dinucleotide; ATP, adenosine triphosphate. Every circle represents a molecule.
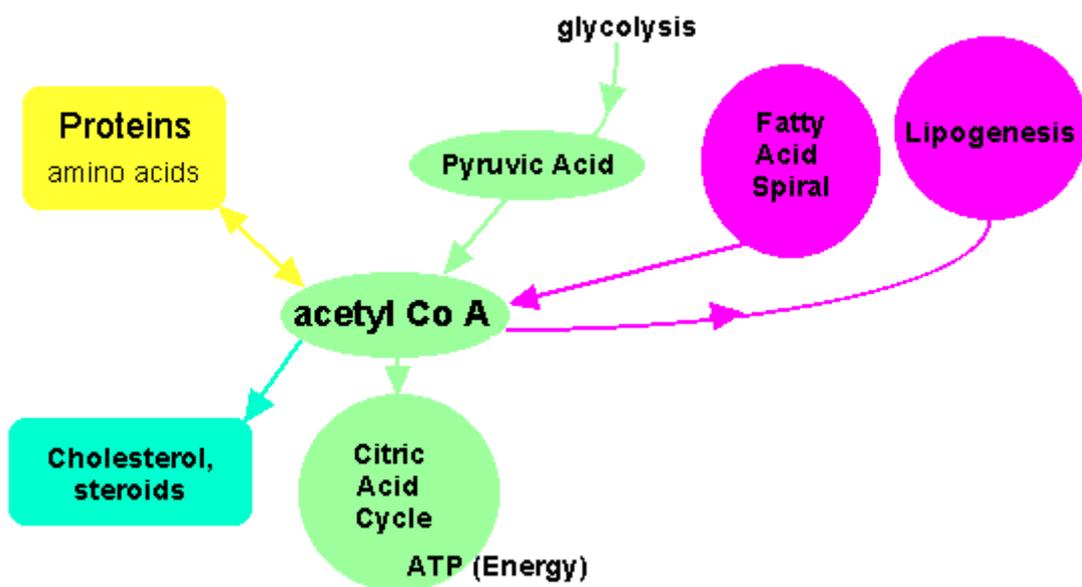
Figure 3 : Illustration of the central role of acetyl-CoA in cellular metabolism. [11]

1.4   Capillary Zone Electrophoresis

The separation of highly polar compounds in reversed-phase HPLC is limited by a lack of retention. CE is a powerful analytical tool for the analysis of charged species.

The apparent mobility of an analyte is the vector sum of the electrophoretic mobility and of the electroosmotic flow:

$$\mu_{app} = \mu_{ep} \pm \mu_{eo}$$

with μ_{app}, apparent mobility; μ_{ep} ionic mobility; μ_{eo}, electroosmotic mobility.

The electrophoretic mobility is a function of the electric field strength the analyte's ionic charge and size. Thus, anions tend to migrate toward the anode while cations tend to migrate toward the cathode (Figure 4).
The electroosmotic flow (EOF) occurs because of the surface charge on the wall of the capillary (zeta potential). In a fused silica capillary the silanol groups are negatively charged at pH values greater than 2 [12]. The cations of the buffer act as conterions, thus resulting in an electric double layer.
When a voltage is applied, the mobile positive charges migrate in the direction of the cathode. All the fluid in the capillary is then dragged along by the migrating positive charges.
The EOF is then generated uniformly down the entire length of the capillary resulting in a flat flow profile. Thus, capillary electrophoresis generally operates with more theoretical plates than HPLC, which is characterized by a laminar flow, providing peak broadering.
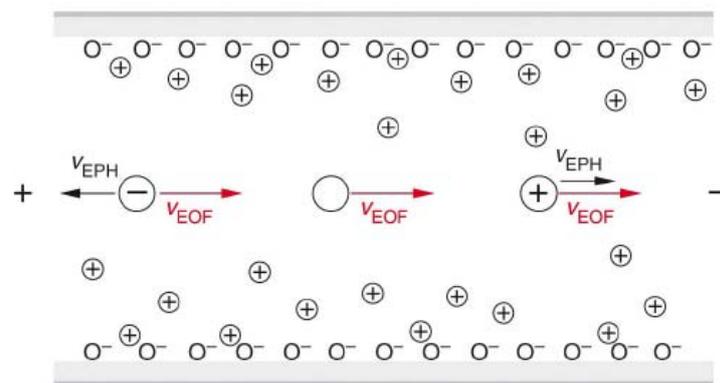
Aus Lottspeich/Engels, *Bioanalytik*, 2. Aufl., © 2006 Elsevier GmbH

Figure 4 : Influence of the EOF and the electrophoretic velocity (V_{EPH}) on an anion, a neutral particle and a cation in a fused silica capillary. [13]

1.5   Challenges in analyzing anionic compounds in CE-MS mode

Usually the analysis of anions by CE is performed in negative mode (where the inlet of the capillary is at the cathode and the outlet at the anode). However, in CE/ESI-MS mode there is no outlet vial. Thus an EOF movement toward the cathode (opposite the MS direction) would create a gap in the liquid at the capillary exit, thus resulting in a current drop (Figure 5 A).
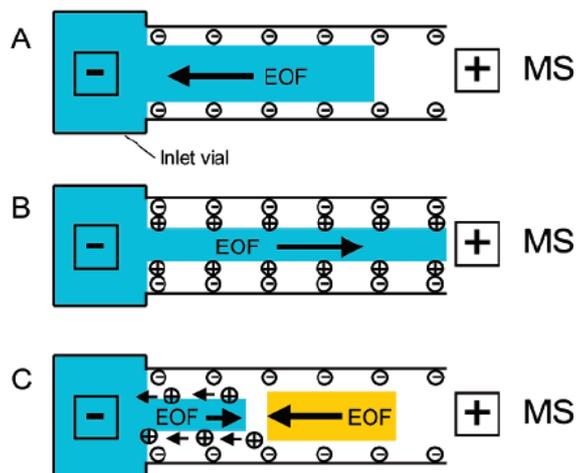
Figure 5 : Schematic depiction of the EOF profile in CE-MS with negative mode. (A) Normal EOF, (B) EOF reversal with a cationic coated capillary, (C) EOF reversal by addition of cationic surfactant to the electrolyte and production of no-liquid zone by generating normal EOF. [14]

A feasible approach for the analysis of anionic compounds by CE-MS is to use a coated capillary with a positively charged surface [4] [12], which creates a permanent EOF toward the anode (MS side),as illustrated in Figure 5 B. Unfortunately, this elegant solution presents several disadvantages: the expense of coated capillaries, the limited pH range and the short lifetime compared with uncoated fused-silica capillaries [15].

An alternative method to reverse the EOF would be the addition of a cationic surfactant to the buffer. However, it has been reported that a current drop was invariably observed [14]. A current hypothesis assumes that the cationic surfactant on the wall of the capillary also migrates toward the cathode (inlet vial), as illustrated by Figure 5 C.

Another alternative is to use a noncharged polymer capillary [16]. With this method all anions migrate toward the MS side by their electrophoretic mobilities. However, it has been reported [15] that, when using polydimethylsiloxane-coated capillaries, the EOF was still observed to migrate toward the cathode (inlet), thus resulting in a current drop.

A fourth alternative method would be to employ a conventional fused-silica capillary with an alkaline running buffer solution in positive polarity mode.

The apparent mobility of the target analyte corresponds to the vector sum of the electroosmotic flow (EOF) and the analyte's electrophoretic mobility. If the EOF flow rate is greater than the electrophoretic mobilites of the analytes, the direction of apparent mobilites of the anions would be toward the cathode. This would allow anionic compounds to be analyzed using CE-MS.

When the pH of the running buffer solution is above 9 the electroosmotic mobility is sufficiently high [17] that the solute's net migration is toward the negative electrode. For example, *H. Sawada et al.* [15] take advantage of the EOF toward the cathode and report the separation of small carboxylic acids. *T. Soga et al.* [18] report the analysis of nucleotides using this alternative method.

In analogy to these earlier studies, the present work proposes a capillary electrophoresis qTOF mass spectrometry (CE-MS) method for the analysis of anionic metabolites under alkaline pH conditions using a normal fused-silica capillary column, as illustrated in Figure 6.
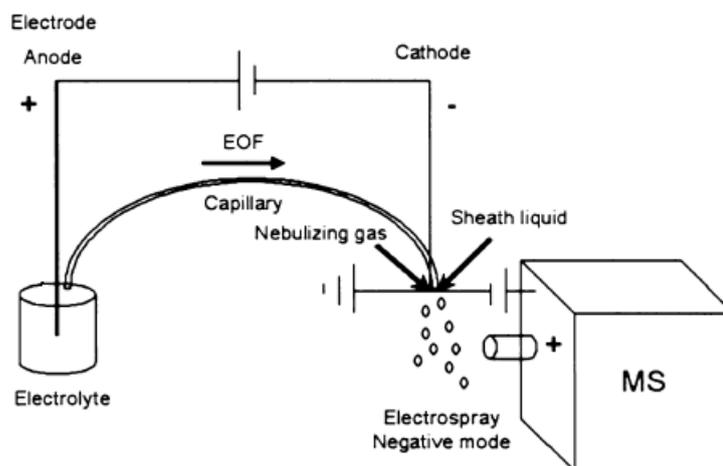
Figure 6 : CE-MS in alkaline buffer conditions with conventional fused-silica capillary for the analysed of anionic compounds. [18]

1.6 Quadrupole-Time of Flight (qTOF) tandem mass spectrometry

The qTOF instrument is operated as a tandem MS which means that two MSs are operated in series. The first MS serves as a filter to transmit only the selected parent ions. These ions may then be fragmented in a collision cell and the resulting fragmented ions are analyzed by the second mass spectrometer. This analytical method allows the very specific detection of ions and their fragments with very high mass accuracy. The analysis of fragmentation patterns provides valuable structural information about analytes.

The QTOF instrument can also work in MS mode, as operated in this work. In this case, mass data are acquired without the collision gas. All parameters are set as for MS/MS but the collision energy is kept very low to avoid fragmentation [19].

The design of the QTOF tandem mass spectrometer is illustrated by Figure 7.

Ions are sampled from the atmospheric pressure electrospray ionization source though the first octopole ion guide into the Quadrupole Mass Filter (Q_1). Both octupoles are operated in radio frequency mode. The potential created by the radio-frequency-field provides radial confinement of the precursor and fragment ions.

Q_1 is operated in the mass filter mode to transmit only the parent ions of interest. Ions selected by the quadrupole are then passed into the collision cell where ions undergo collisions with neutral gas molecules (nitrogen).

The resulting fragment ions are then focused by the second octopole and focused by lenses. The ions enter into the Time-of-Flight analyzer as a parallel beam. A high voltage pulse is applied to start the flight of the ions into the flight tube. Finally, ions are deflected by the ion mirror to the detector made of microchannel plates. Electrons escape to begin the process of the electrical signal reads by the data system. [19] [20]
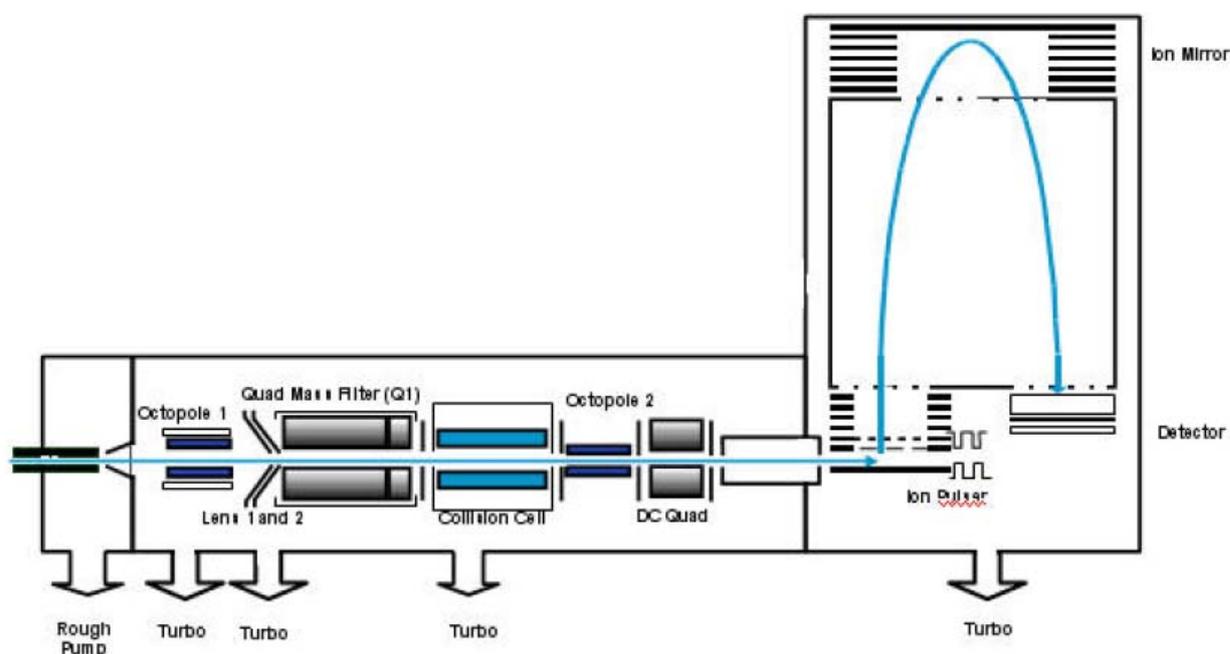
Figure 7 : Schematic outline of the Agilent QTOF mass spectrometer [20]

The mass to charge ratio of each ion correlates directly with its flight time in the flight tube. Collision between ion and residual gas will affect the accuracy of the mass calibration [20]. Hence, a very low level of vacuum must be supplied (from an extra turbo pump) to the QTOF to prevent any ion collision.

1.7   Coupling capillary electrophoresis to mass spectrometry

Coupling CE to the ion source of a MS instrument requires an electrical contact in the absence of an outlet reservoir and the generation of a sufficient flow to keep the spray stable.
This can be accomplished using a sheath-flow interface (Figure 8).
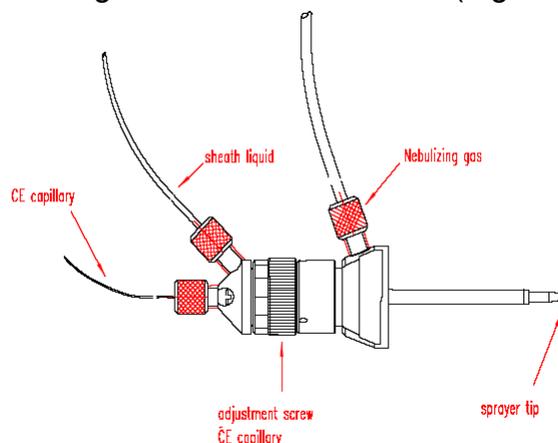
Figure 8 : CE-ESI-MS Sprayer, Agilent design [21]

The CE-ESI-MS provides a coaxial sheath liquid which adjusts the flow rate generated by the CE (1 to 50 nL/min [12]) to the compatible flow rate of the electrospray interface (5 to 50 µL/min [12]).
The tip of the capillary on the MS side works like an electrode being grounded along with the electrospray [17] and the sheath liquid while serving as an outlet buffer vial.

The sheath liquid around the outside of the capillary provides a stable electrical connection between the tip of the capillary and the grounded electrospray. [5]

2 Experimental

2.1 Chemicals and reagents

Buffer / Sheath liquid / capillary Preconditioning				
Name	**Acronym**	**Purity**	**Origin**	**Warning** [www.chemexper.com]
Ammonium formate CH_5NO_2	AmFor	99.995+ %	Sigma-Aldrich 51691-100G	Irritating to eyes, respiratory system and skin
Ammonium hydroxide NH_3	-	Trace Metal Grade	Fisher Scientific Lot n° 7108100	Causes burns, very toxic for aquatic organisms
Water H_2O	H_2O	High purity Solvent for Gas chromatography, HPLC and Spectrometry	Burdick & Jackson Cat NP365-10	No warning
Methanol CH_3OH	MeOH	99.9+%	Burdick & Jackson Cat 230-4	Highly flammable, toxic by inhalation, in contact with skin and if swallowed danger of very serious irreversible effects
Sodium hydroxide solution 1 N NaOH for CE separation	NaOH	Not provided	Agilent Technologies Lot ZC742568526	Causes severe burns
API-TOF Reference	-		Agilent Technologies G1969-85001	
Tuning mix ES-TOF	-		Agilent Technologies G 1969-85000	Toxic and Flammable, one ion known to cause cancer
Reference Standards				
Name	**Acronym**	**Purity**	**Origin**	**Warning** [www.chemexper.com]
Citric acid $C_6H_8O_7$	-	Not provided	Sigma Lot 21K0042	Irritating to eyes respiratory system and skin
Malic acid disodium salt $C_4H_4O_5Na_2$	-	Min. 95%	Sigma Lot 38H1383	Irritating to respiratory system and skin
Succinic acid $C_4H_6O_4$	-	Min. 99%	Sigma Lot 121K0028	Avoid contact with skin and eyes
Malonic acid $C_3H_4O_4$	-	Not provided	Sigma Lot 073K3608	Harmful by inhalation and if swallowed, irritating to respiratory system and skin
Dihydroxyacetone phosphate dilithium salt $C_3H_5Li_2O_6P$	DHAP	Min. 95%	Sigma D-7137	

D-Fructose 1,6-bisphosphate tetra(cyclohexyl-ammonium) salt $C_6H_{14}O_{12}P_2 \cdot 4C_6H_{13}N$	FBP	Min. 95%	Sigma F-0752	
D-Fructose 6-phosphate disodium salt hydrate $C_6H_{11}Na_2O_9P \cdot xH_2O$	F6P	~98%	Sigma F-3627	Harmful by inhalation, in contact with skin and if swallowed; possible risk of irreversible effects
D-Glucose 6-phosphate disodium salt hydrate $C_6H_{11}Na_2O_9P$	G6P	98-100%	Sigma G-7250	
D-(-)-3-Phosphoglyceric acid Disodium salt $C_3H_5Na_2O_7P$	PGA	~95%	Sigma P-8877	Harmful by inhalation, in contact with skin and if swallowed; possible risk of irreversible effects
D-Ribose 5-phosphate Disodium salt hydrate $C_5H_9Na_2O_8P \cdot xH_2O$	R5P	Min. 98%	Sigma R-7750	
D-Ribulose 1,5-bisphosphate sodium salt hydrate $C_5H_{12}O_{11}P_2 \cdot Na^+ yH_2O$	RuBP	~90%	Sigma R-0878	Toxic by inhalation, in contact with skin and if swallowed
Coenzyme A Trilitium salt trihydrate $C_{23}H_{35}N_7O_{17}P_3SLi_3 \cdot 3H_2O$	CoA	96+%	MP Biomedicals Inc. lot 2603J	Avoid contact with skin and eyes
Acetyl coenzyme A Sodium salt $C_{23}H_{38}N_7O_{17}P_3S \cdot xNa^+$	Acetyl-CoA	Min. 94%	Sigma A2056	
Malonyl coenzyme A lithium salt $C_{24}H_{38}N_7O_{19}P_3S \cdot xLi^+$	Malonyl-CoA	Min. 90%	Sigma M-4414	
Isobutyryl coenzyme A $C_{25}H_{42}N_7O_{17}P_3S \cdot xLi^+$	Isobutyryl-CoA	Min 85%	Sigma I-0383	
Propionyl coenzyme A lithium salt	Propionyl-CoA	Min. 85%	Sigma P-5397	
β-hydroxybutyryl coenzyme A lithium salt $C_{25}H_{42}N_7O_{18}P_3S \cdot xLi^+$	β-hydroxybutyryl-CoA	Min. 90%	Sigma H-0261	
3-Hydroxy-3methylglutaryl coenzyme A sodium salt $C_{27}H_{44}N_7O_{20}P_3S \cdot xNa^+$	HMG-CoA	Min. 90 %	Sigma H-6132	
Butyryl coenzyme A lithium salt hydrate $C_{25}H_{42}N_7O_{17}P_3S \cdot xLi^+ \cdot yH2O$	Butyryl-CoA	Min. 90%	Sigma B-1508	

2.2   Instrumentation

G1602A Agilent CE Instrument
G6510AA LC/MSD TOF, ESI source
G2226A 1200 Series Nanoflow Pump
G1607 CE-ESI-MS sprayer kit

Agilent ChemStation for CE System Software   Rev. B. 03. 01
Agilent MassHunter Workstation Software   Version B.02.00
Agilent MassHunter DataAcquisition Software   Version B.01.03

CE-MS cassette
CE capillary: 50μm fused silica capillary with polyimide coating (Polymicro Technologies TSP050375)
Capillary Column Cutter with Rotating Diamond Blade

Vial crimp7snap, polypropylene 1ml, Agilent technologies
Insert tube 100 μl insert, polypropylene, Agilent technologies
Snap cap polyurethane, Agilent technologies

Infuser xdScientific
Syringe infuser 1 ml Agilent Technologies

pH meter 430, Corning (relative accuracy: ± 0.01)
Ultrason bath Fisher Scientific FS30H

2.3   Preparation of solutions

2.3.1 Buffers

The buffer solutions were prepared by diluting the AmFor salt in high purity water.
The pH value was adjusted with 0.9 N NaOH solution.
Before being used, solutions were filtered though a nylon filter (0.2 μm) and placed in an ultrasonic bath to remove air bubbles.

2.3.2 Standards

For the development of separation methods for anionic metabolites, stock solutions of authentic standards were prepared in water.

Table 1 : Stock solutions of organic acids

Organic acids	Weighted mass [mg]	Dilution volume [ml]	$M_{stock\ solution}$ [mol/l]	$m_{stock\ solution}$ [mg/l]
Citric acid	24.6	25	$5.12*10^{-3}$	984
Malic acid	33.5	25	$7.52*10^{-3}$	1340
Succinic acid	25.7	25	$8.70*10^{-3}$	1028
Malonic acid	28.0	25	$1.07*10^{-2}$	1120

Table 2 : Stock solutions of coenzymes A derivatives

Coenzymes A	Weighted mass [mg]	Dilution volume [ml]	$M_{stock solution}$ [mol/l]	$m_{stock solution}$ [mg/l]
CoA	~1	8	$1.6*10^{-4}$	125
Acetyl-CoA	~1	8	$1.5*10^{-4}$	125
Malonyl-CoA				100
Isobutyl-CoA	Provided by H. Chen, J. Browse Lab			100
Propionyl-CoA	Solution were made by diluting compounds in di			100
B-hydroxybutyloyl-CoA	deionised water			100
HMG-CoA				100

Stock solutions of sugar phosphates had been prepared in 2006 as reported by C. Emery, in her Diploma thesis entitled *Metabolic profiling of sugar phosphates using HPLC-MS with mixed-mode stationary phases*, and had been stored at -20°C.

Table 3 : Stock solutions of sugar phosphates

Sugar phosphates	$M_{stock solution}$ [mol/l]	$m_{stock solution}$ [mg/l]
G6P	$8.22*10^{-3}$	23.2
F6P	$8.55*10^{-3}$	26.0
R5P	$8.54*10^{-3}$	23.4
DHAP	$8.30*10^{-3}$	15.1
PGA	$8.35*10^{-3}$	19.2
FBP	$3.94*10^{-3}$	29.0
RuBP	$4.68*10^{-3}$	18.8

Each solution was filtered using a nylon filter (0.2 µm) before being injected in the CE-MS.
When not in use, all authentic standard solutions were stored at -20°C.

2.3.3 Sheath liquid

4 µl/min of (0.44:0.44:0.088:0.032) MeOH:H_2O:NH_3:API TOF Reference solution was delivered to the CE interface to provide a sufficient flow rate and an electrical contact to the outlet tip of the capillary.
Ammonium hydroxide was added to facilitate the ionization and methanol to increase the nebulization.
Reference solution was added to maintain a perpetual calibration of the MS.

2.4 CE method

Because the diameter of the capillaries was small (50 µm) and the buffer volatile, the capillary was very sensitive to clogging especially at the MS tip because of temperature variation of the gas nebulizer. Thus, the capillary length was reduced several times during this work by cutting off the clogged portion of the capillary.

Everyday, before running any samples, an Ohm's law plot was established by filling the capillary with the buffer, varying the voltage, recording the current and plotting the results. Runs were operated on the linear portion of the curve as illustrated in Figure 9. Operating on the linear portion of the curve generally yields the highest number of theoretical plates and provides a better reproducibility between runs. Indeed, when a conduction of electric current though an electrolytic solution, heat is generated by collision between ions, called Joule heating. This may result in the formation of a radial thermal gradient and temperature changes between runs. [17]
The Ohm's law plot provides the control of heat dissipation, by a variation of the slope, highlighting resistance fluctuations, which is a function of the conductivity, which is itself a function of the temperature.
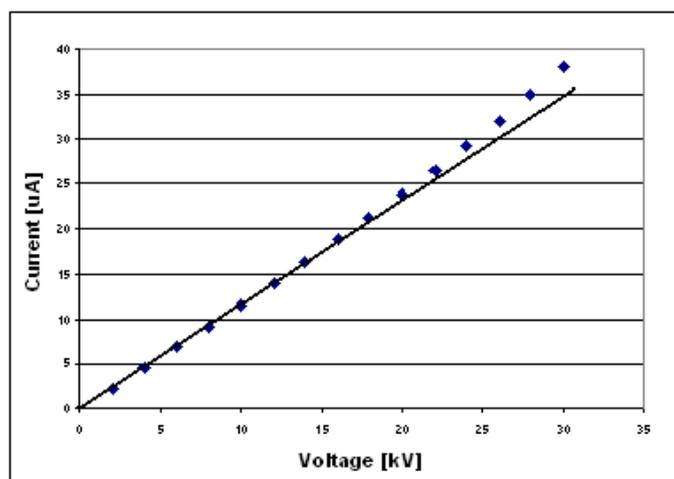
Figure 9 : Example of a daily Ohm's law plot. The run was operated at 18kV in that case.

The connection between the CE and the mass spectrometer was only established by the fused-bare capillary, which left the CE cassette to rich the ESI source of the MS as shown in Figure 10.
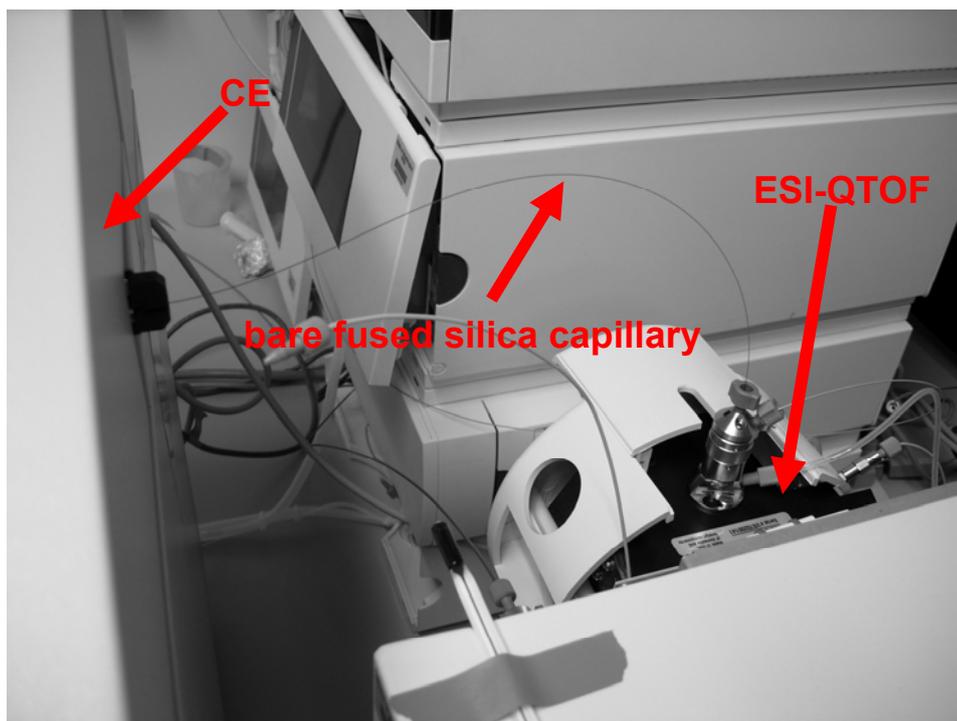
Figure 10 : Interface between CE and ESI-QTOF, connected with the bare fused silica capillary.

The design of the coupling was in such that, the first part of capillary was temperature-controlled (set at 25°C) and the second part was exposed to room temperature. The temperature along the capillary was assumed to be the same as the standard room temperature 25°C. However, consistency of temperature of the second part of capillary was actually difficult to maintain due to the variation of room temperature, and therefore caused fluctuations of migration time. Moreover, the slight differences in temperature between two parts of capillary might have negative effect on the efficiency of separation. The lack of cooling system on the second part of capillary might decrease the efficiency of separation as well, by preventing the forced convection process of heat production and thus increasing the thermal gradient in the capillary in the second part of the capillary.

To avoid a siphoning effect, the CE was placed so that the CE inlet vial was at the same height as the sprayer tip of the mass spectrometer.

For all runs certain CE parameters that remained constant are listed in Table 4.

Table 4 : Constant CE parameters, except if mentioned:

Parameters	Values	
Pressure injection	50 mbar	} ~ 10 nl volume injected
Time injection	8 sec	
Voltage ramp	1min	
Separation mode	positive	
Cassette temperature	25°C	
Composition of sheath liquid	(0.44:0.44:0.088:0.032)MeOH:H_2O:NH_3:API TOF Reference solution	
Flow of sheath liquid	4 µl/min	
Preconditioning of capillary before each run	Flush with 5 min NaOH/ 5 min water/ 10 min buffer	

To assess the efficiency of the separation, the number of theoretical plates were calculated according to Equ. 1, which is based on Einstein diffusion equation and on the definition of theoretical plates *N*, given by Equ. 2.

$$N = \frac{\mu_{ep}U}{2D_m}$$

Equ. 1

$$N = \frac{L^2}{\sigma_T^2}$$

Equ. 2

Equ 1 requires the assumption that diffusion is the only source of peak broadening [17]. When analyzing our own CE-MS data with Equ 1, peaks with noticeable broadening had sometimes better efficiencies than peaks with good symmetry. This means that another source of peak broadening, besides diffusion, took place during the separation.

One main factor contributing to the dispersion can be the variations in temperature along the capillary (as mentioned previously).
Peak broadening might also be caused by a certain injection volume [22]. Indeed, to apply Equ. 1, the sample is assumed to be present as an infinitely thin zone which is an unrealistic assumption. In reality, the injection has a finite zone and hence will influence the overall band dispersion. Second, sample solution is assumed to enter the capillary as a rectangular plug, which is not the case when the sample is injected directly onto the capillary [22]. Moreover, siphoning can also be a cause of peak shape inconsistencies particularly in the CE-MS design, where the height between inlet and outlet is difficult to adjust.

Equ. 3 appeared to provide more meaningful results than the traditional efficiency calculation given in Equ. 1, although this approach is used primarily for liquid chromatography.

$$N = 2\pi \frac{h_p^2 L^2}{A_p^2}$$

Equ. 3

where A_p is the area of the peak [intensity*sec], h_p is the height of the peak [intensity], and L the distance traveled by the peak [sec].

This method allowed the determination of σ_T^2, the total variance of the dispersive phenomenon from experimental data, based on Equ. 2. But, it has to be taken into consideration that this method is based on measurements of the standard deviation of a Gaussian peak. In capillary electrophoresis, peaks are not Gaussian. Thus, Equ. 3 provides only an estimate of the efficiency.
In regular CE mode, because the detection occurs on-capillary and because migration velocity of each solute through the capillary is a function of its electrophoretic mobility, a correction factor must be applied to normalize peak area. Indeed slower moving components spend more time migrating past the detector window than the more rapidly moving compounds, which increases the peak area counts of slow moving components. But since detection was performed postcapillary in CE-MS mode, the correction of peak area normalization was eliminated. A_p was then used for the calculation of N and was taken directly from integration report (the software did not apply a correction automatically).

2.5 MS method

MS parameters that were kept constant during this project are listed in Table 5. The following parameters were used before the optimization of the detector response for Malonyl-CoA.

Table 5 : Constant parameter

Parameters	Values
Ionization mode	Negative
Drying gas flow	4 l/min
Drying Gas Temperature	250°C
Nebulizer pressure	6 psi
Capillary voltage	3000V
Mass Range	106-1000
Acquisition Rate/Time	9652
Fragmentor voltage	150V
Skimmer voltage	65V
Octopoles voltage	750V

2.6 Overview of analyses

CE-MS mode:

Metabolite group	Concentration of each metabolite in sample	Migration conditions	Detection conditions	Data files
Citric acid solution	~10 mg/l	Without preconditioning Running buffer : 20mM AmFor (pH = 9.75) Capillary : 50µm x 70 cm Applied voltage : 18 kV	ESI-negative	organicacid056.d to 059.d
Citric acid solution	~10 mg/l	Running buffer : 20mM AmFor (pH = 9.75) Capillary : 50µm x 70 cm Applied voltage : 20 kV	ESI-negative	organicacid060.d to 062.d & organicacid066.d to 067.d
Mix organic acids	~10 mg/l	Running buffer : 20mM AmFor (pH = 9.75) Capillary : 50µm x 70 cm Applied voltage : 20 kV	ESI-negative	organicacid073.d to 077.d
Citric acid solution	~10 mg/l	Run during several days Running buffer : 20mM AmFor (pH = 9.75) Capillary : 50µm x 70 cm Applied voltage : 20 kV	ESI-negative	organicacid063.d to 081.d
Mix sugar phosphate	~2 mg/l	Running buffer : 20mM AmFor (pH = 9.75) Capillary : 50µm x 65 cm Applied voltage : 20 kV	ESI-negative	oraganicacid083.d & sugarphosphate003.d
Mix sugar phosphate	~1 mg/l	Running buffer : 20mM AmFor (pH = 9.75) Capillary : 50µm x 65 cm Applied voltage : 20 kV	ESI-negative	sugarphosphate004.d to 006.d
Mix sugar phosphate	~1 mg/l	Running buffer : 25mM AmFor (pH = 9.75) Capillary : 50µm x 65 cm Applied voltage : 20 kV	ESI-negative	sugarphosphate007.d
Mix coenzymes A	~10 mg/l	Running buffer : 25mM AmFor (pH = 9.75) Capillary : 50µm x 68 cm Applied voltage : 15 kV	ESI-negative	CoA033.d to 036.d
CoA, Acetyl-CoA and Malonyl-CoA	~10 mg/l	Running buffer : 25mM AmFor (pH = 9.75) Capillary : 50µm x 71 cm Applied voltage : 20 kV	ESI-negative	CoA015.d to 018
Detector response Malonyl-CoA	~1 mg/l	Direct infusion into MS	ESI negative and positive	optiCoA000.d to 030.d
Test extraction with standard solution	~ 5mg/l	Running buffer : 25mM AmFor (pH = 9.75) Capillary : 50µm x 65 cm Applied voltage : 20 kV	ESI-positive and Negative	CoA100.d and CoA104.d to 105.d

CE-UV mode :

Metabolite group	Concentration of each metabolite in sample	Migration conditions	Detection conditions	Data files
Mix coenzymes A	10 mg/l	Injection 50mbar, 20sec (~25nl) Running buffer : 25mM AmFor (pH = 9.75) Capillary : L_T= 62 cm / L_D= 53.5 Applied voltage :18 kV Positive mode separation	256.50 nm	8CoA_004.d to 008.d
Extract concentrated		Injection 50mbar, 20sec (~25nl) Running buffer : 25mM AmFor (pH = 9.75) Capillary : L_T= 62 cm / L_D= 53.5 cm Applied voltage : 18kV Positive mode separation	256.50 nm	CeExtract003.d
Mix coenzyme A just after true simple	10 mg/l	Without preconditioning capillary Injection 50mbar, 20sec (~25nl) Running buffer : 25mM AmFor (pH = 9.75) Capillary : L_T= 62 cm / L_D= 53.5 cm Applied voltage : 18kV Positive mode separation	256.50 nm	8CoA_009.d

3   Results and discussion

The first step in operating the CE-MS was to establish a valid connection between the CE and the MS and the softwares, and replicate the separation of the quinine sample, according to the constructor's instructions.
Connectivity and mutual recognition of the two instruments was established by a number of cables joining the computer, the QTOF, the CE and the nanopump involving several assays to figure out how to activate the connection between instruments.
Besides, CE-MS operation involved two distinct softwares. These two softwares, however, were not initially designed to work in combination since the coupling of CE-QTOF has never been attempted previously and is a world first.
Hence, controlling both softwares and obtaining the hardwares mutual recognition in order to run the instruments in parallel was challenging.

Then, in order to establish a reference, it was attempted to reproduce a previously reported method for the separation of anionic metabolites.
Very few papers reported a separation using bare fused-silica capillaries in positive mode separation for anionic compounds. *H. Sawada et al.* [15] utilized such separation conditions for the analysis of carboxylic acids. For the current study, the first experiments were thus chosen to be performed with a standard solution of citric acid, the organic acid reported to have the longest migration time and the most problematic peak symmetry.

The MS interface restricts the choice of CE buffers to volatile types. Furthermore, their concentrations must be kept low to allow efficient ion production [5] and the pH must be alkaline in order to reach a sufficiently high EOF flow.
Separations, according to [15], were carried out in 20 mM ammonium formate buffer adjusted to pH 10. AmFor is a good candidate for a CE buffer because of its volatile properties and its wide buffering capacity in the alkaline range (8.2-10.2 [23]).

Samples were prepared in water or in the running buffer to evaluate buffer effects on peak symmetry. The base peak width was almost 2 min when the analyte was diluted in running buffer, which decreased to 0.2 min in water, Figure 11.
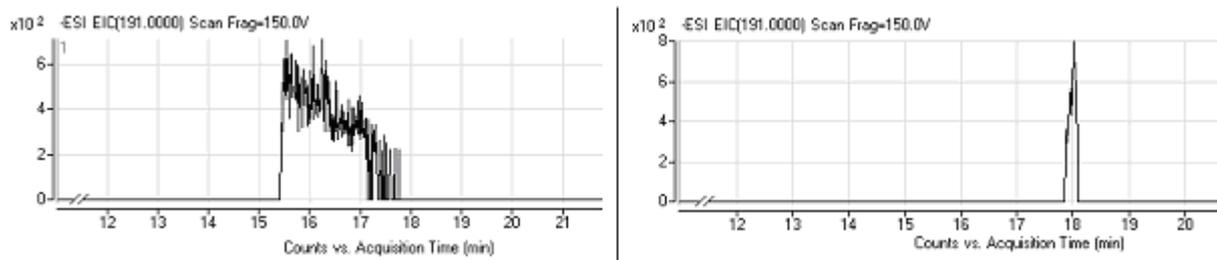
Figure 11 : Effect of sample buffer on peak symmetry. On the left, the sample was diluted in running buffer (1.3 ρmol injected), on the right the sample was diluted in water (0.78 ρmol injected).

This phenomenon is a result of a conductivity difference between the injection solution and buffer solution. As a consequence of Ohm's law, the sample diluted in water generates a higher field strength in the injection zone compared to the remainder of

the capillary. The negatively charged solutes migrate out of the injection zone towards the anode and encounters the buffer zone where the field strength abruptly drops. The electrophoretic velocity of the solutes slows and anions stack in the boundary between the injection solution and buffer solution thus resulting in a compression of the solute zone, a process known as stacking (Figure 12). [17]

When the sample was diluted in running buffer this process did not occur because the conductivity of the injection zone and buffer zone was the same.

Thus, the sample has to be prepared in a solution with higher field strength than the capillary solution. Thus, all samples were then diluted in water.
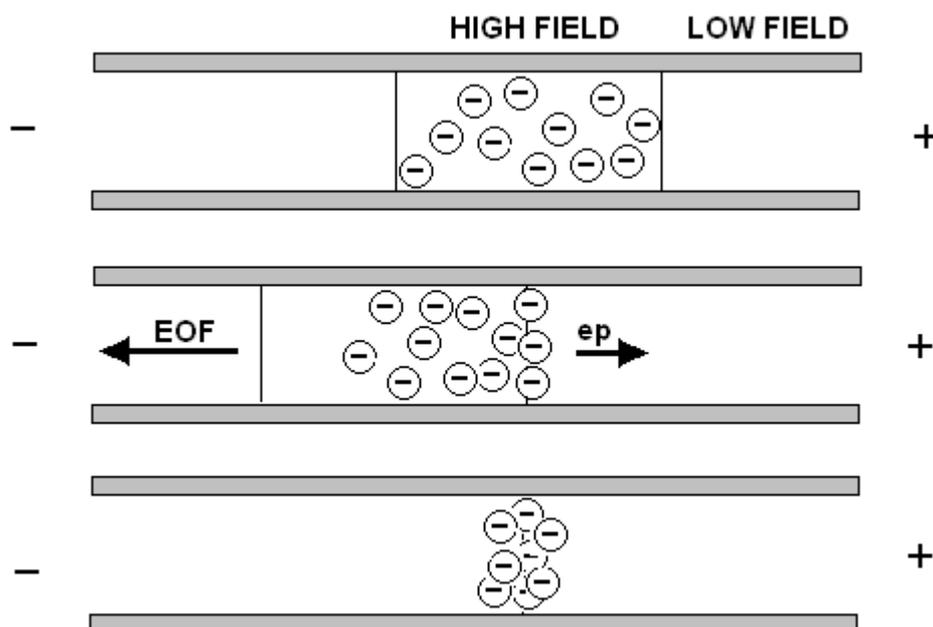
Figure 12 : Illustration of stacking of anions under alkaline-pH buffer conditions, ep: electrophoretic mobility

In capillary electrophoresis, electrolysis occurs at both electrodes, thus resulting in pH changes [17]. Since the pH is one of the most important experimental parameters in capillary electrophoresis, with particularly high impact on the EOF and migration time drift [17], its effect must be minimized by replacing the buffer frequently. Despite of replacing the buffer after each run, the repeatability of the migration time was relatively poor, with a relative standard deviation (R.S.D.) of 18.7 % (n=4). The R.S.D. of the migration time was reduced to 1.1 % (n=5) when a flushing cycle preceded each run (5 min of 1 N NaOH solution and 5 min of Water).

After these first optimization steps, conditions for the separation of several groups of anionic compounds were tested.

3.1   Separation of organic acids

Using the same conditions as for the citric acid separation, a standard solution of four organic acids ~ 10 mg/l (citric acid, succinic acid, malonic acid and malic acid) was tested. The achieved separation is illustrated by the electropherograms shown in Figure 13.
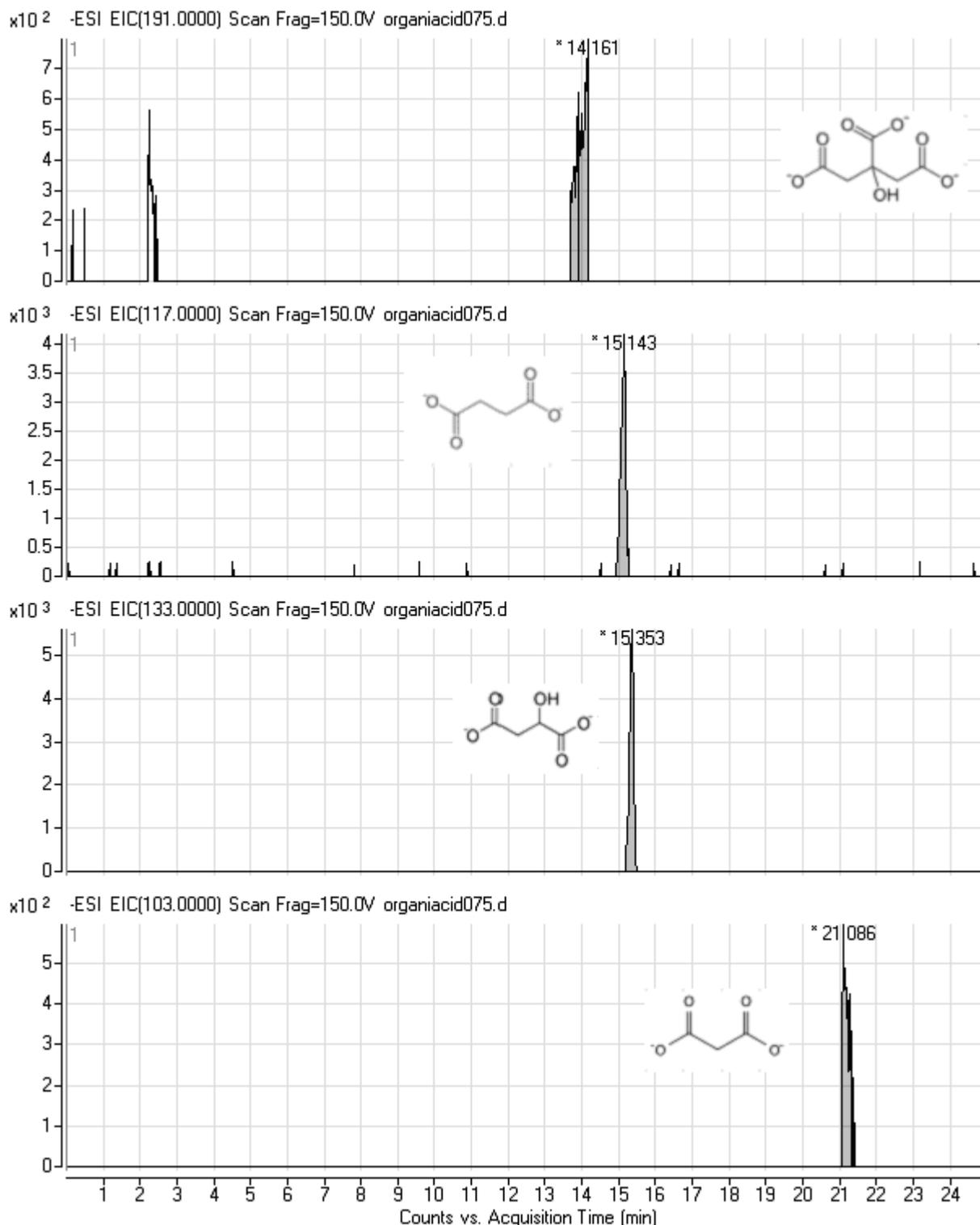
Figure 13 : Extracted ions electropherogram of a standard mix of organic acids (~ 10 mg/l citric acid ([M-H]⁻=191), succinic acid ([M-H]⁻=117), malic acid ([M-H]⁻=133), malonic acid ([M-H]⁻=103))

Extracted ions have been obtained by selecting the [M-H]⁻ of each compound. Deprotonated ions were observed as the most abundant ion under the examined condition.

The efficiency of the organic acids separation is presented by Table 6, bringing to light the poor shape peak of citric acid.

Table 6 : efficiency of the separation calculated with Eq. 1 and standard deviation calculated by doing the average for each N, [a] n=5, [b] n=3

	Efficiency N	S.D
citric acid[a]	13227	± 2734
succinic acid[a]	58386	± 3930
malic acid[a]	85639	± 11734
malonic acid[b]	82020	± 13817

Assays were run to assess the reproducibility of the separation of this organic acid mix.
Standard deviation (S. D.) values for the migration time of the organic acids separation are summarized in Table 7.

Table 7 : Standard deviation values of the migration time for each organic acids, n=5 except for malonic acid n=3

	Migration time [min]	S.D. Migration time [min]
citric acid	14.01	0.18
succinic acid	15.06	0.20
malic acid	15.26	0.19
malonic acid	21.06	0.39

The standard deviation values were less than 0.2 min for three of the carboxylic acids. The S.D is a lightly higher for the malonic acid migration time, probably because of the small assay number.
These small variations of migration time were acceptable. However standard deviations become important when comparing data acquired on different days. Day-to-day variations of up to 4 min were recorded. Fluctuations of ± 2°C were measured in the room as well as current variations of ± 2 µA between days. This means that migration times for each analyte need to be determined every day before samples are processed.

Despite migration time fluctuations between days, three divalent organic acids were separated with good peak symmetry (Figure 13). The poor shape of the malonic acid peak arose from the low detector response for this anion. Furthermore, the trivalent carboxylic acid, citrate was expected to elute with a higher migration time compared to the other organic acids [15]. To better understand the reasons of this difference, the citric acid, from the same stock solution, was run again, under the same conditions. It was discovered that the migration time was shifted, resulting in a more reasonable migration time order regarding to the charge and the mass of the metabolite (Figure 14). Moreover the peak shape was much better. The calculated efficiency was 90862

in that case. This shift of the citric acid when diluted with other organic acids does not find an explanation.
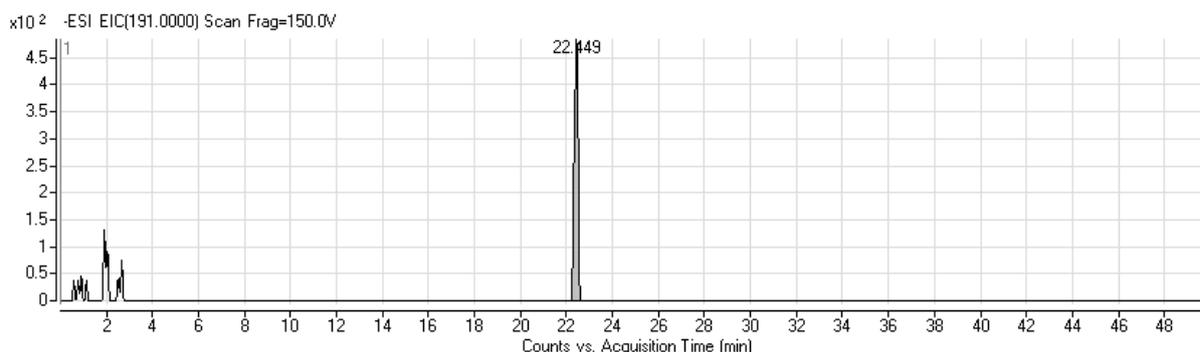
Figure 14 : Extracted ion electropherogram of citric acid (~ 10 mg/l), with exact same conditions than previously operated with the mix of organic acids.

3.2   Separation of sugar phosphates

With the aim of ultimately developing a method for simultaneous separation of different groups of anionic metabolites, a standard solution of 7 sugars phosphates ~1mg/l (G6P, F6P, R5P, DHAP, PGA, FBP and RuBP) was then tested under the same conditions as the organic acids mix.

Six of the seven sugar phosphates were well separated, only G6P and F6P co-migrated. However, peak broadening was observed for certain sugar phosphates. To minimize electrodispersion, the sample was diluted and the buffer concentration increased. Separation efficiency factors were then plotted as a function of these parameters in Figure 15.
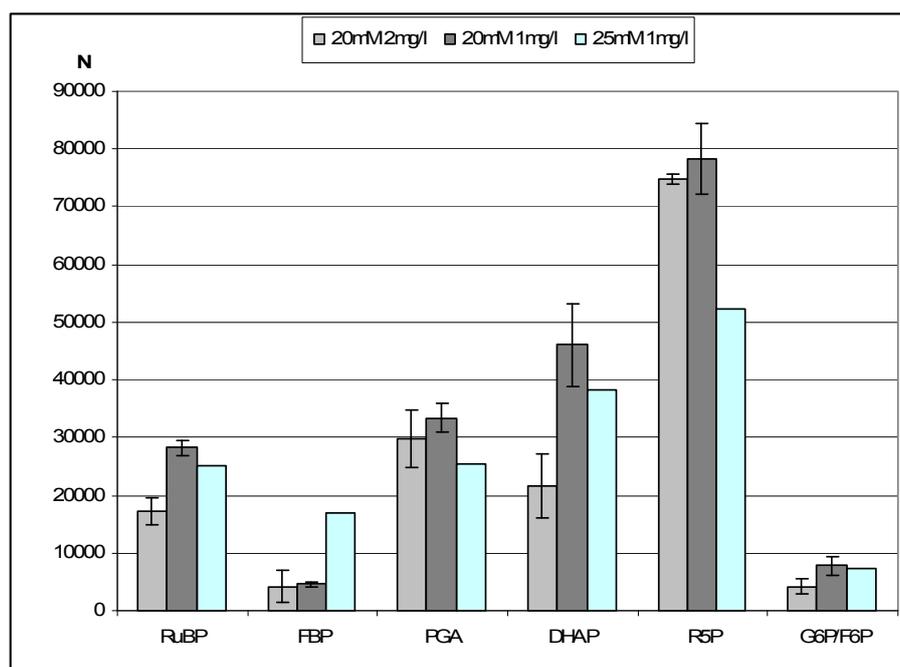
Figure 15 : Plot of the efficiency for each sugar phosphate under different conditions.

The dilution of the sample seemed to confer better efficiency for the separation, pariculary for RuBP, DHAP and G6P/F6P. The dilution of the sample might provide a higher field strength within the area of injection compared to the remainder of the capillary thus favoring the stacking process. Contrary to expectations, increasing the buffer concentration did not improve the number of theoretical plates under the examined conditions, except for FBP with an improvement of almost 50%. The buffer concentration differences were probably not sufficient to achieve a significant effect on the separation efficiency. Later on a broader range of buffer concentrations as well as pHs were tested but uncontrollable current fluctuations occurred, thus preventing any data processing.

The electropherograms of the separation, run at 25mM running buffer are shown in Figure 16.

The migration order of the sugar phosphates was as expected. The first metabolite reaching the detector was the one with the most diluted charge: a high number of carbons and one phosphate group (G6P and F6P). Then smaller sugar phosphates with one phosphate group (R5P and DHAP), metabolites with two phosphate groups (FBP and RuBP) and finally the smallest sugar phosphate with a carboxylic function (PGA) eluted.

The F6P and G6P peaks overlapped. Since the CE separation is based on the charge and size of ionic species, the two isomers migrated at the same time with a same charge and the same molecular weight. The use of a SMILE (+) capillary tended to increase the separation of these isomers, without achieving a complete separation [14]. In our case the use of the EOF to achieve the separation in a bare fused silica capillary does not demonstrate a satisfactory separation for these two isomers.
Besides the overlap of the isomers F6P and G6P, our new method separated sugar phosphates with satisfactory resolution. A previously developed reversed-phase HPLC method achieved a partial separation of G6P and F6P, but overlapping peaks of F6P, R5P and DHAP was reported [10].
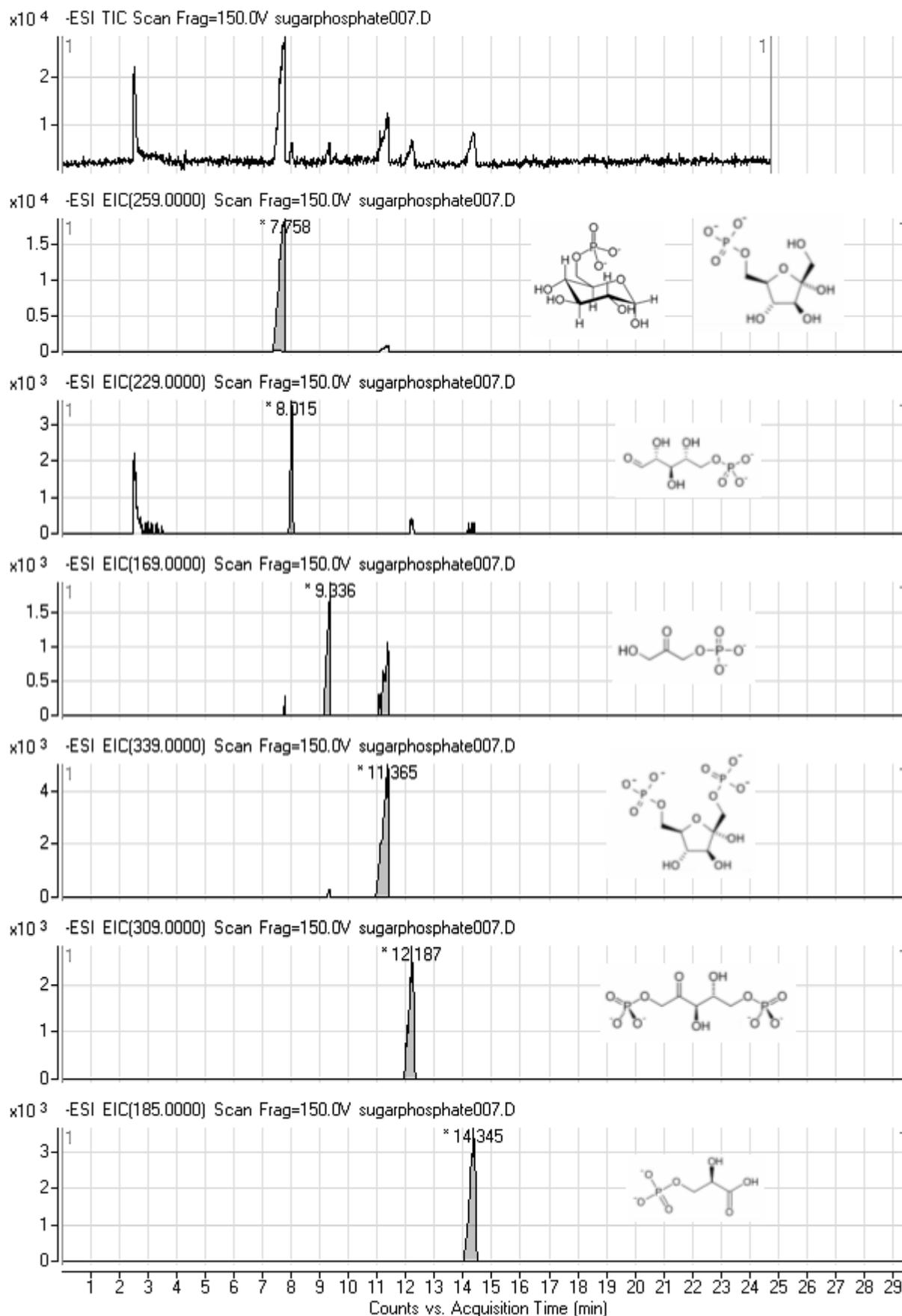
Figure 16 : Total ion current and extracted ion electropherograms of the ~1mg/l standard solution of G6P/F6P[M-H]⁻=259, R5P [M-H]⁻=229, DHAP [M-H]⁻=169, FBP [M-H]⁻=339, RuBP [M-H]⁻=309 and PGA [M-H]⁻=185.

A method using a cationic coated capillary (SMILE(+)), which is approximately one hundred times more expensive, provides a similar separation, with the exact inverse migration order [4]. The reproducibility of migration times with our bare fused silica capillary was more than sufficient when the recorded current was stable, as shown Table 8.

Table 8 : Standard deviation of sugar phosphate migration times based on tree runs.

	Migration time [min]	S.D. Migration time [min]
G6P/F6P	7.24	0.13
R5P	7.47	0.11
DHAP	8.54	0.13
FBP	10.02	0.20
RuBP	10.80	0.07
PGA	12.22	0.01

Under these conditions, deprotonated ions of each sugar phosphate were observed as the most abundant ion, as shown in Figure 17. However with G6P or F6P, DHAP, PGA and FBP dimers ([2-M-H]$^-$) were detected in addition to parent ions with the respective m/z of 518.9; 338.9; 370.9 and 678.9. The loss of a phosphate (m/z= 79) was detected as well, as the most important fragmentation (m/z 184.9-80=104.9; m/z 338.9-80=258.9). The adduct of a Na to the parent ion ([M-1+Na]$^-$) and to the dimer ([2-M-H+2Na]$^-$) were frequently observed too (m/z 308.9+22=330.9 ; m/z 184.9+22=206.9; its dimer m/z 370.9+22=392.9; m/z 168.9+22=190.9 and its dimer m/z 338.9+22=360.9).

Some of the smaller peaks visible in the electropherograms in Figure 16 were due to the fragmentation of sugar phosphates. Table 9 summarizes the presumed nature of the different peaks according to their migration times and their m/z.

Table 9 : Presumed nature of small peaks observed in sugar phosphate electropherograms.

Migration time [min]	m/z	presumed origin
11.365	259	m/z 339-80, loss of a phosphate from FBP
12.187	229	m/z 309-80, loss of a phosphate from RuBP
14.345	229	m/z 185+2*22, two Na adduct of PGA
11.365	169	m/z 339-170, alkyl fragmentation of FBP
8.015	229	m/z 259-91, alkyl fragmentation
9.336	339	m/z (2*170)-1, DHAP dimer
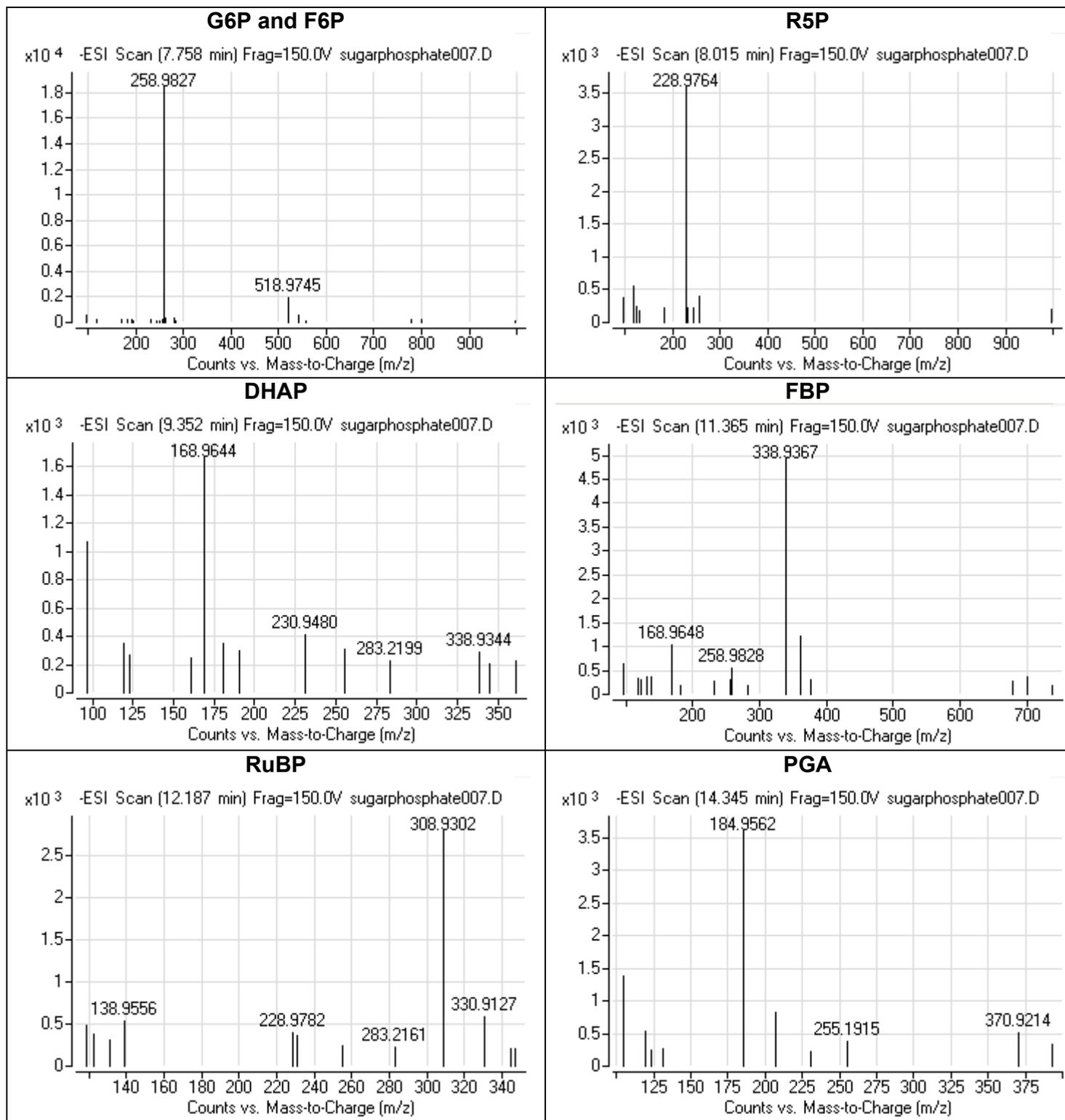
Figure 17 : ESI-TOF mass spectra for sugar phosphates.

3.3   Separation of coenzyme A derivatives

A standard solution of 8 coenzyme A derivatives (~ 10 mg/l) was run under the same conditions as the sugar phosphate separation.
CoA, acetyl-CoA, malonyl-CoA, β-hydroxybutyryl-CoA, propionyl-CoA and HMG-CoA were completely separated, as shown in Figure 18. Isobutyryl-CoA and butyryl-CoA co-migrated. The co-migration of these two isomers was expected, with such similar structures and identical charge.
Malonyl-CoA and β-hydroxybutyryl-CoA, which have the same m/z, were distinguished by running each compound individually. The fragmentation spectra did not allow the distinction of these two isobar metabolites because of the high similarity of their structures.

The standard deviations of migration times as well as symmetry of the peaks and efficiency values for the separation of CoA derivatives were very promising (Table 10 and Table 11).

Table 10 : Migration time and standard deviation established with four consecutive runs with a standard solution of ~ 10 mg/l of each coenzyme A derivative.

	Migration time [min]	**S.D. Migration time [min]**
β-hydroxybutyryl-CoA	12.517	0.51
Isobutyryl-CoA/ Butyryl-CoA	12.678	0.54
Propionyl-CoA	12.737	0.65
Acetyl-CoA	12.947	0.56
CoA	13.581	0.79
HMG-CoA	13.892	0.78
Manoyl-CoA	14.067	1.14

Table 11 : Average efficiency factors, based on tree consecutive runs.

	Efficiency	
β-hydroxybutyryl-CoA	181386	± 67354
Isobutyryl-CoA/ Butyryl-CoA	185896	± 70830
Propionyl-CoA	162140	± 52371
Acetyl-CoA	176125	± 50747
CoA	285445	±138040
HMG-CoA	192742	± 70271
Manoyl-CoA	188701	± 49354
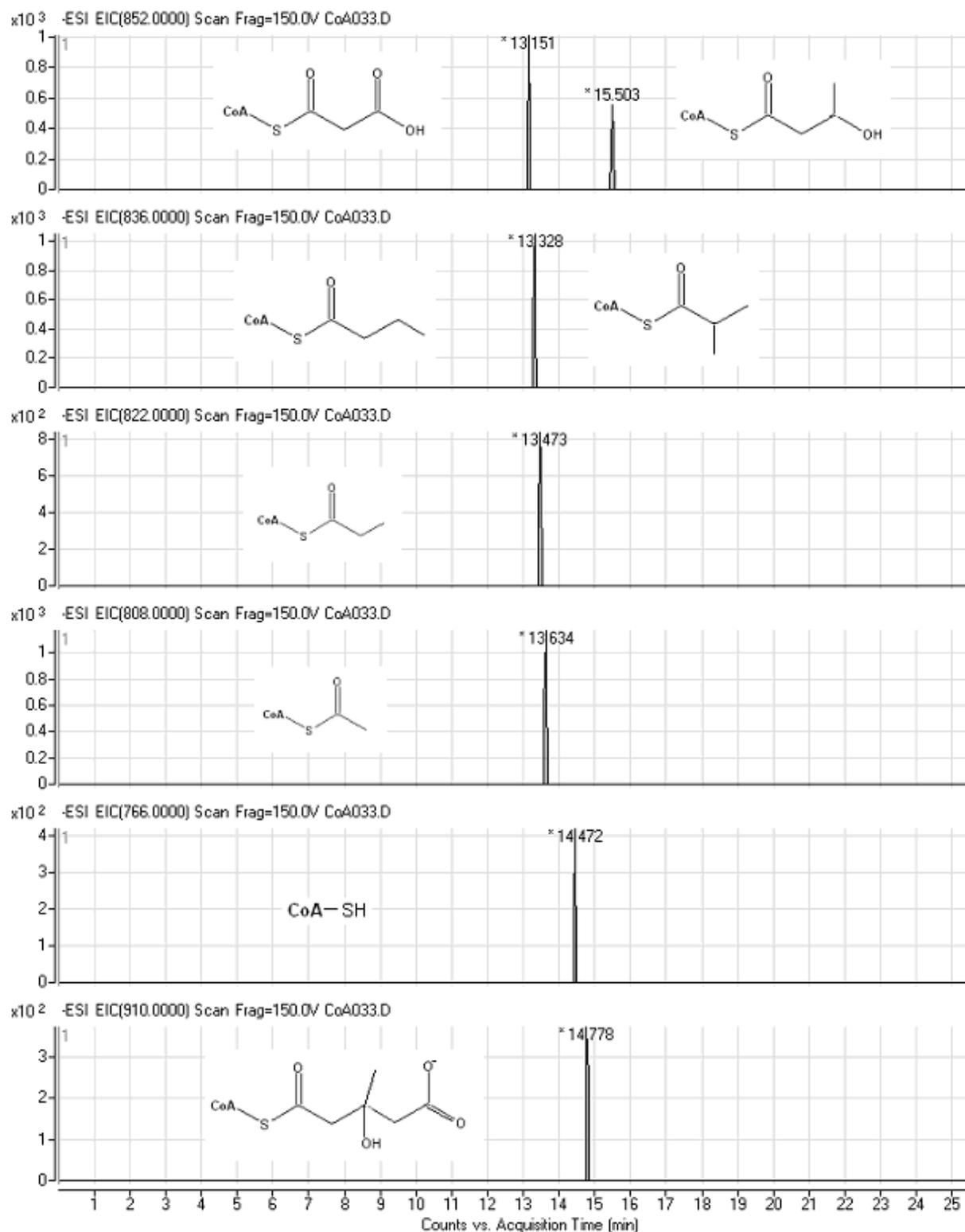
Figure 18 : Single ion traces for [M-H]⁻ 852 (Malonyl-CoA and β-hydroxybutyryl-CoA) , 836 (Isobutyryl-CoA/Butyryl-CoA), 822 (Propionyl-CoA), 808 (Acetyl-CoA), 766 (CoA), 910 (HMG-CoA).

Moreover, this is the first study reporting on the separation and detection of a mix of coenzyme A derivatives by CE-MS. The technique described here allows for an unambiguous and sensitive analysis of these important cellular metabolites.

A CE diode array method has been reported [9] with a sodium phosphate buffer and a fused-silica capillary but this method does not allow to probe the identity of compounds because of the highly similar UV/VIS spectra of all CoA derivatives.

With this promising separation, the decision was then made to focus the project on the detection of coenzyme A derivatives in a biological sample. Extractions were performed with *Arabidopsis thaliana L* leaves.

According to literature the concentration in *A. thaliana* of coenzyme A is reported between 10pmol/g [24] and 5nmol/g [25]. The detection in such low concentrations of coenzyme A derivatives arose to be a new challenge. Indeed their detection turned out to be difficult, compare to sugar phosphate. For example, when ~ 32 fmol of RuBP were injected, a signal with an intensity of $\sim3\cdot10^3$ was recorded while a signal of $\sim4\cdot10^2$ was recorded for CoA, when ~130 fmol were injected.

Since the detection of coenzymes A was poor, optimization of the detector response and optimization of the extraction method were carried out in parallel in order to allow the detection of coenzyme A derivatives in *A. thaliana* leave tissue.

3.3.1   *Optimization of detector response*

The optimization was preformed by direct infusion of the malonyl-CoA into the MS by varying each parameter, presented inTable 12, one by one manually.

Malonyl-CoA was chosen for the optimization of the detector response because it is a good representative of coenzyme A derivatives.

The solution composition infused in the MS had to match the conditions present when the coenzyme A derivatives eluted from the CE separation. Thus, a solution of 1mg/l of malonyl-CoA in 0.45:0.45:0.1 $MeOH:H_2O:NH_3$ was prepared to reproduce the separation conditions. The solution was infused in the ESI-TOF with a flow rate of 284 µl/h with an infuser xdScientific and a 1ml infuser-syringe.

The first optimized parameter was the mode of electrospray ionization. Ion currents were acquired in positive and negative mode. Positive mode was found to give a signal almost two times better than negative mode.

We observed then, that to set the quadrupole mass filter of QTOF by selecting the $[M-H]^+$ of the parent ion, without collision energy, increased the intensity of the signal. This ion filtration step increased the sensibility of the detection of ~ 40%.

Finally the parameters reported in Table 12 were varying one by one and the optimal values provided a signal five times better than previously.

Table 12 : QTOF optimal values parameters for malonyl-CoA detection

Parameters	Values
Ionization mode	positive
Drying gas flow	4 l/min
Drying Gas Temperature	250°C
Nebulizer pressure	4 psig
Capillary voltage	4500 V
Fragmentor voltage	200 V
Skimmer voltage	65 V
Octopoles voltage	750 V

For each optimization experiment, the malonyl-CoA solution was infused for 1 min. The signal intensities of the molecular peak were recorded five times during each run in order to get an average signal intensity.

The optimal value for the gas temperature was initially 325°C. However, at this temperature, the buffer in the tip of the capillary evaporated, thus resulting in a current drop. A temperature of 250°C for the gas temperature was found to be a good compromise.

3.3.2   True sample

In order to achieve the detection of a really low range concentration for the coenzyme A derivatives, different extraction methods were tried to access to a sample which provided a detectable concentration and an appropriate viscosity allowing the injection. Those two requirements were theoretically reach with the extraction method reported by *J. A. Cruz et al.* [10] for the sugar phosphates [Appendix A].

After improving the detector response for the specific metabolites as well as finding the extraction method enabling a concentration step of the sample, runs failed to detect the metabolites. This is because electrical current in capillary inevitably collapsed whenever the analyses were performed, therefore the efficiency of the extraction method could not be verified.

After current collapse was consistently observed, the extract was then run in CE-UV mode, to see if the same problem was accoutred. A stable current was recorded all the run long. Unfortunately several compounds UV absorbent in much higher concentration than coenzymes A migrated with the same migration time [CeExtract003.d], preventing to the detection of coenzyme A derivatives by this method.

Finally trials were attempted in CE-MS mode again, with the standard solution and a new capillary to re-establish a baseline. But the current drop was still observed preventing result as previously observed.

3.4   Troubleshooting

Because the CE-MS coupling is a recent technique and because this project was the first using this instrument in the lab, several difficulties were encountered.
The complete troubleshooting record for this project is available in [Appendix B]

During this project, it was found that the positioning of the capillary tip in the CE-ESI-MS sprayer kit (outside protruding length of the CE capillary tip) was especially important to keep a stable CE current.
When the length was too long it was assumed that the drop in the current resulted from a short circuit with the ESI interface. But on the other hand when the tip length was too short, reduced sensitivity was observed. A larger nebulization cone was generated under such conditions, decreasing the number of ions entering into the MS.
The optimal protruding length was found by turning the adjustment screw 1.5 marks in the clockwise instead of 2 marks as suggested in the instructions of the User's Guide [21].

Drops in the CE current, illustrated in Figure 19, were also observed because of capillary clogging. When the instrument was not in use, standby mode was set automatically; the drying gas heated up to 300°C and led to evaporation of water in the capillary resulting in current drops. To prevent this problem, the nebulizer kit was removed when the QTOF was put into standby mode.

Appling a voltage ramp instead of a full voltage at the beginning of the run, had also been observed to prevent current collapses. Indeed, instead of applied a full voltage at once, the software allowed to set a ramp voltage to rich the required voltage which was observed to decrease the current drop effects.

However, current collapse occurred more frequently after the injection of true sample. To troubleshoot the problem, several parameters were investigated.
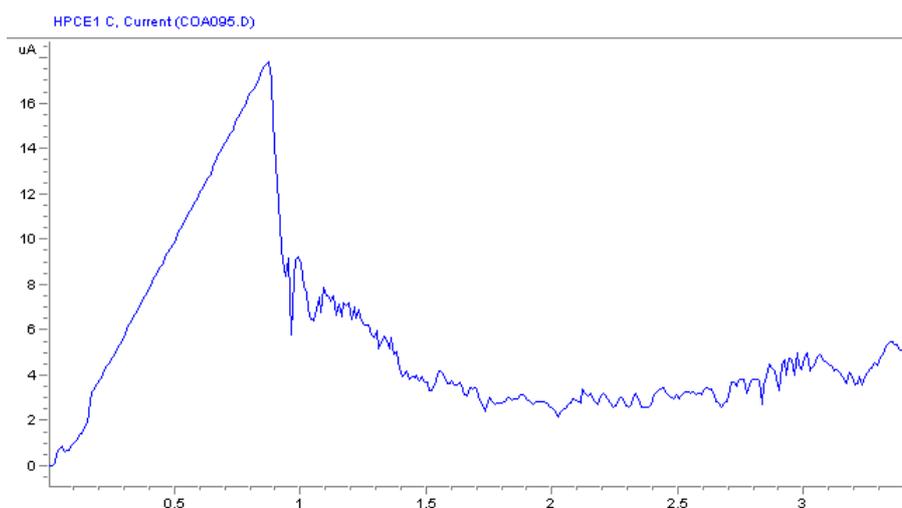
Figure 19: Illustration of a typical current drop problem.

Buffer precipitates, dust and other solid material in the electrodes had been reported [21] to cause arcing or current leakage. Thus the electrode and the nebulizer kit were

cleaned regularly with high purity isopropanol but the frequency of current drops was not decresed by this measure.

To evaluate if current drops were caused by a faulty design of the CE-MS interference kit, the separation of coenzyme A derivatives was performed in CE-UV mode, illustrated in Figure 20.
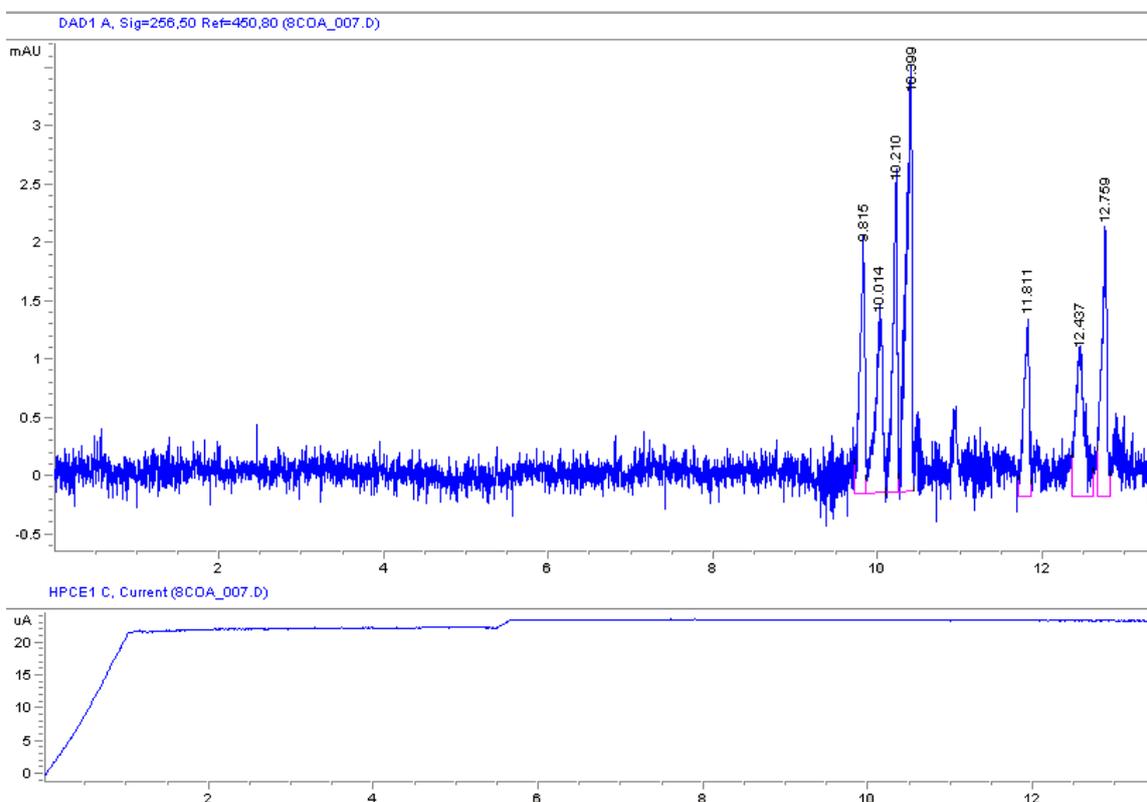
Figure 20 : Electropherogram of ~10mg/l coenzyme A derivatives mix detected at 256.50 nm in CE mode (at the top) as well as stable recorded current (bottom).

Interestingly, no more current drops were observed not even with than fifteen injections. It was then tested if the recurrent current drops in CE-MS mode also occurred under condition where the electrophoretic and electroosmotic flow were both in the direction of the MS. A solution of four amino acids (10mg/l) was tested with the same condition than anionic metabolites but using a 1M formic acid buffer, in negative and positive ionization mode, and a sheath liquid made of 1:1 (5mM formic acid:MeOH). But the same problem with the current drop was still observed.

The following other parameters were tried, all without success: methanol was substituted by isopropanol in order to provide a higher viscosity to the sheath liquid, increasing the electrical connection to complete the CE electrical circuit. Voltage setting parameter was investigated by switching the voltage from high to low and vice versa. Similar testing was conducted on ionization modes as well, by switching the positive and negative modes. However, all the attempts made were in vain and current collapse problem persisted. In fact, this problem had also been encountered by other research groups who are working on CE-MS as well. For instance, *M. Hashimoto et al.* [26] reported similar trouble as us and come up with the fabrication of their own electrospray interface.

4 Conclusions

After a promising beginning with the separation of various anionic metabolites, further method development was frustrated by frequent current drops, the source of which could not be resolved.

However the method did produce promising results with an inexpensive and durable capillary.

A method was established to provide a separation of sugar phosphates with a bare fused silica capillary which in the past was only reported with an expensive and short lived life coated capillary.

Moreover it is the first time that coenzyme A derivatives have been reported to be separated by CE-MS. This novel separation of such central metabolites may allow for advances in the understanding of metabolic process in the future.

5 Acknowledgments

Dr. B. Mark Lange, for being a helpful supervisor and giving me the opportunity to first use the CE-qTOF technique,

Dr. Matthias Wüst, for offering me the opportunity to conduct the experience for my thesis at Washington State University,

The Bureau MOVE of HES-SO Valais for providing me with a scholarship,

All the members of the Lange Laboratory for their support and a welcoming working environment,

All my friends in Pullman, for an enjoyable experience off work,

Siau Sie and Tim for their constant support,

Thank you!

Diploma thesis carried out in Washington State University, submitted in HES-SO-Valais, Sion, March 2009.

Cindy Meyrat

6 References

[1]   D. Ryan & K. Robards, Metabolomics: The Greatest Omics of Them All?, Analytical Chemistry, **78**, (2006), p. 7954-7958

[2]   L. W. Sumner, P. Mendes, R. A. Dixon, Plant metabolomics : large-scale phytochemistry in the functional genomics era, Phytochemistry, **62**, (2003), p. 817-836

[3]   R. Bhalla, K. Narasimhan, S. Swarup, Metabolomics and its role in understanding cellular responses in plants, Plan Cell, **24**, (2005), p.562-571

[4]   S. Sato, T. Soga, T. Nishioka & M. Tomita, Simultaneous determination of the main metabolites in rice leaves using capillary electrophoresis mass spectrometriy and capillary electrophoresis diode array detection, The Plant Journal, **40,** (2004), p. 151-163

[5]   M. R. N. Monton & T. Soga, Metabolome analysis by capillary eletrophoresis-mass spectrometry, Journal of Chromatography, **1168**, (2007), p.237-246

[6]   R. Ramautra, A. Demirci & G. J. de Jong, Capillary electrophoresis in metabolomics, Trends in Analytical Chemistry, **25**, (2006), p. 455-466

[7]   M.R.N Monton & T. Soga, Editorial on « Metabolome analysis by cabillary electrophoresis-mass spectrometry », Journal of Chromatography, **1168**, (2007), p.236

[8]   N. A . Campbell & J. B. Reece, *Biology*, Eignth Edition, Pearson Benjamin Cummings, San Fransisco, (2007)

[9]   G. Liu, J. Chen, P. Che & Y. Ma, Separation and quantification of short-chain coenzyme A's in biological sample by capillary electrophoresis, Analytical Chemistry, **75**, (2003), p. 78-82

[10]   J. A. Cruz, C. Emery, M. Wüst, D. M. Kramer & B. M. Lange, Metabolite profillg of the Calvin cycle intermediates by HPLC-MS using mixed-mode stationary phases, The Plant Journal, **55**, (2008), p. 1047-1060

[11]   Acetyl-CoA Cross Roads Compouds, http://www.elmhurst.edu/~chm/vchembook/623acetylCoAfate.html

[12]   M. Taverna, I. Le Potier & P. Morin, Electrophorèse capillaire , in F. Durieux & *all*, Technique de l'ingénieur, Technique de l'ingénieur, Paris, (1982), P 3365 - P 3366 – P 3367

[13]   F. Lottspeich & J. W. Engels, Bioanalytik, 2 Auflage, Elsevier, GmbH, Münich, (2006)

[14]   T. Soga, Y. Uneno, H. Naraoka, Y. Ohashi, M. Tomita & T. Nishioka, Simultanenous Determination of Anionic Intermediates for *Bacillus subtilis* Metabolic Pathways by Capillary Electrophoresis Electrospray Ionization Mass Spectrometry, Analytical Chemistry, **74**, (2002), p. 2233-2239

[15]   H. Sawada & C. Nogami, Capillary electrophoresis-electrospray ionization mass spectrometry using uncoated fused-silica capillaries and alkaline buffer solution for analysis of small carboxylic acids, Analytica Chimica Acta, **507**, (2004), p.191-198

[16]   T. Soga, Y. Uneno, H. Naraoka, Y. Ohashi, M. Tomita & T. Nishioka, Pressure-Assisted Capillary Electrophoresis Electrospray Ionization Mass Spectrometry for Ananlysis of Multivalent Anions, Analytical Chemistry, **74**, (2002), p. 6224-6229

[17]   R. Weinberger, *Practical Capillary Electrophoresis*, Second Edition, Academic Press, San Diego, (2000)

[18]   T. Soga, T. Ishikawa, S. Igarashi, K. Sugawara, Y. Kakazu & M. Tomita, Analysis of nucleotides by pressure-assisted capillary electrophoresis-mass spectrometry using combination of polarity reversion and electroosmotic flow for metabolomics Anion Analysis, Journal of Chromatography, **1159**, (2007), p.125-133

[19]   I. V. Chernushevich, A. V. Loboda & B. A. Thomson, An introduction to quadrupole-time-of-flight mass spectrometry, Journal of masse spectrometry, **36**, (2001), p. 849-865

[20]   Agilent 6200 Series TOF and 6500 Series Q-TOF LC/MS System, Concept Guide, (2007)

[21]   Agilent Capillary Electrophoresis System, User's Guide, Part No G1600-90009, (2204)

[22]   P. D. Grossman & J. C. Colburn, *Capillary Electrophoresis Theory and Practice*, First Edition, Academic Press, San Diego, (1992)

[23]   ACE HPLC Columns, Technical Report PB04041, Optimizing Reversed Phase HPLC Separation fot High Throughput Applications, http://www.mac-mod.com/tr/04041-tr.html

[24]   T. R. Larson & I. A. Graham, A novel technique for the sensitive quantification of CoA esters from plant tissues, The Plant Journal, **25**, (2001), p. 115-125

[25]   A. W. Tumaney, J. B. Ohlrogge & M. Pollard, Acetyl coenzyme A concentrations in plant tissues, J. Plant Physiology, **161**, (2004), p.485-488

[26]   M. Hashimoto, Y. Ishihama, M. Tomita & T. Soga, Microelectrospay interface with coaxial sheath flow for high-resolution capillary electrophoresis/mass spectrometry separation, Mass Spectrometry, **21**, (2007), p. 3579-3584

7 Appendix

Appendix A   Extraction Method

Appendix B   Troubleshooting

Appendix A

Extraction Method:

J. A. Cruz, C. Emery, M. Wüst, D. Kramer, B. M. Lange, *Metabolite profiling of Calvin cycle intermedicates by HPLC-MS using mixed-mode stationary phases*, The Plant Journal, **55**, (2008), p.1047-1060

Flash freeze ~ 1 gram leaf tissues in N_2 (liquid) and grind in an N2 (liquid) cooled mortar.
Transfer powdered leaf tissues to 5ml of MeOH:$CHCl_3$:formic acid:H_2O 12:5:1:2 (v/v) (R. L. Bieleski, The problem of halting enzyme action when extracting plant tissues, Analytical Biochemistry, **9**, p.431-442) pre-chilled to -20°C.
Add 1.96 ml of ice-cold $CHCl_3$ and 2.8 ml of ice-cold water.
Centrifuge at 3225 rcf for 10 min at 4°C
The suspension separates into tree distinct layers : an unpper aqueous phase and a lower organic phase separated by a curd layer containing insolubles.
Transfer the aqueous phase to a pear-shaped flask
Carefully drain the organic phase from the centrifuge tube. Extract the remaining curd layer twice with 2ml 1% formic acid and 20% methanol (aq,v/v), using low speed spins (2000 rcf 7 min) to pellet the insolubles.
Pool the supernatants with the aqueous phase from the previous step

Filter the pooled fraction through a disposable serum filter to remove large particulates

Concentrate pooled fractions by mild rotary evaporation (for ~45min at 35°C)

Reconstitue with 1ml water
Spin final solutionin a microcentriguge to pellet insolubles
Pass the sample through a preparatory cation exchange filter to remove contaminating cations (Strata-X-C 33µm Polymeric Strong Cation, Phenomenex, 8B-S029-TBJ)

Evaporate the fraction to dryness and reconstitute with 100ul of water

Filter the sample through a 0.25µm filter

Appendix B

Troubleshooting

Current

	Possible cause	Comment
instability	not enough liquid in the vial	make sure that the electrod is in the liquid
	capillary not in the nebulizer	
bizarre noise	capillary broken	erratic current
current drop	capillary broken	erratic current
	capillary clogged	cut the tip of the capillary that is inserted into the MS side
		do not set MS in standby when the nebulizer is installed
	readjust the capillary in the nebulizer	Most of the time, the current is more stable if the adjustment scew is tuned 1.5 mark clockwise
	build a voltage ramp instead of a full voltage	

Broken capillary

	Possible cause	Comment
broken capillary	when the exterior coating of the capillary touches solvent	exterior polyimide coating prevent capillary failure, do not clean the capillary with acetone as advised in the user manual of Capillary Cutter, it becomes fragile and breaks

Error Message CE chemstation

	Possible cause	Comment
fan off	make sure that the cassette is moved back	there is a problem with the sensor
	open and close the top cover until the error message disappears	
top cover opened	open and close the top cover until the error message disappears	appears each time when CE Chemstation is restarted

Manipulations

	Possible cause	Comment
Preparing the capillary	used the SGT Capillary Column Cutter	poor cut can decrease the precision of the spray
	ensure precise cut	
	burn both tips of the capillary with a cigarette lighter	
	clean the burnt polymide with a tissue moistened with methanol	

Bypass the UV window detecor in CE-MS

	Possible cause	Comment
	use a short and removed polyamide coated piece of capillary for the UV detection window	
	insert the available capillary into the alignment interface to go straight to the MS	

	Possible cause	Comment
Capillary storage	for one or two days : flush with water for 10 min and store with water	
	for more than two days : flush with water and then with emply vial to try the capillary	